Chapter 2

Methodology

2.1 Introduction

Earth's interior is inaccessible, therefore the information about its structure and composition is gathered through indirect means, primarily via measurements of sound velocities during earthquakes[1, 2]. Further, it is now possible to generate the pressure and temperature that prevails within the earth, in the laboratory. Theoretical techniques often serve as a guideline to design future experimental work. Experimentally, the application of pressure is relatively challenging than the application of temperature where the former requires specialized techniques. Usually, pressure is applied to a material using two main high-pressure techniques: static compression methods which use pressure cells, notably diamond anvil cells [59] and dynamic compression methods based on shock waves where the velocity of shock wave generated by a strong shock on the sample is measured [60]. Static compression methods are more accurate than dynamic compression methods, however, the pressure range is limited to the mechanical resistance of a diamond where the upper pressure limit being ∼300 GPa. However, theoretical techniques often come in handy where theoretical predictions can be made for conditions which otherwise impose difficulty in accessing via experimental techniques. Computationally, the application of pressure is straightforward in the framework of density functional theory (DFT) [61] where the unit cell dimension is reduced and the applied pressure can be calculated analytically from the self-consistent one-electron states or from fitting the energy-volume curve by an equation of states to yield the volume derivative of calculated total energy. Unlike simulating

pressure, the effect of temperature is difficult to model as it requires collective vibrations of atoms called phonons. However, theoretical modeling is still necessary for conditions not experimentally accessible. Geophysics often encounters the synergy between experimental and computational approaches. Computational and experimental techniques used in the present thesis work is explored in Section 2.2 and 2.3 respectively.

2.2 Computational Methods

The total energy of a system of electrons and nuclei can be calculated successfully using quantum mechanics. Several properties of the system are associated with the total energy or the difference between the total energy of different configurations. The cell parameters of the crystals are determined by minimizing the total energy of the structure. However, studying the properties of materials on the atomic scale is challenging owing to the presence of complex interactions between electrons and nucleii. This problem is dealt by numerically solving the equations describing a particular situation using computer simulation. Further, the Schrödinger equation can be solved using *ab initio* (first principles) methods which only seeks the atomic number and position of atoms in the crystal structure, without relying on experimental inputs. The initial guess for atomic positions can be obtained from crystal structure prediction methods [62] or from refinement of measured diffraction data. The theoretical study carried out here uses first principles method based on density functional theory (DFT) [61] where a set of equations called Kohn-Sham Equations [63] is solved in a self-consistent manner.

2.2.1 Density functional theory

To predict the geometric and electronic configuration of a material, it is necessary to obtain the total energy by solving the Schrödinger equation and minimize that energy with respect to the nuclear and electronic position. In symbolic terms, any material can be expressed as:

$$\text{material} = \text{nuclei} + \text{electrons}$$

Atoms in crystals are held together by the fine balance between the attractive Coulomb

interactions between nuclei and electrons, and the repulsive interactions between pairs of electrons and pairs of nuclei. The energy associated with Coulomb repulsion between two electrons (V_{ee}) at a distance r_{ee}, the Coulomb repulsion energy between two nuclei (V_{nn}) with atomic number Z at a distance r_{nn} and the energy associated with the Coulomb attraction between an electron and a nucleus (V_{en}) at distance r_{en} are given as:

$$V_{ee} = \frac{e^2}{4\pi\varepsilon_0 r_{ee}} \tag{2.1}$$

$$V_{nn} = \frac{Z^2 e^2}{4\pi\varepsilon_0 r_{nn}} \tag{2.2}$$

$$V_{en} = -\frac{Z^2 e^2}{4\pi\varepsilon_0 r_{en}} \tag{2.3}$$

where e is the electron charge and ε_0 is, the permittivity of vacuum. Restricting the discussion to stationary electronic states, all the properties of the material under study can be determined by solving the time-independent Schrödinger equation:

$$\widehat{H}\psi\left(\mathbf{R}_i;\mathbf{r}_i\right) = E\psi\left(\mathbf{R}_i;\mathbf{r}_i\right) \tag{2.4}$$

where $\psi\left(\mathbf{R}_i;\mathbf{r}_i\right)$ is the wave function describing the quantum state of the system and E is the energy eigen value of the system. Using Equations (2.1)-(2.3), the Hamiltonian describing a material with a set of electrons and nuclei interacting through electrostatic forces can be written as :

$$\begin{aligned}\widehat{H} = -\sum_I \frac{\hbar^2}{2M_I}\nabla_I^2 - \frac{\hbar^2}{2m_e}\sum_i \nabla_i^2 + \frac{1}{2}\sum_{I,J(I\neq J)} \frac{Z_I Z_I e^2}{|\mathbf{R}_I - \mathbf{R}_J|} + \\ \frac{1}{2}\sum_{i,j(i\neq j)} \frac{e^2}{|\mathbf{r}_i - \mathbf{r}_j|} - \frac{1}{2}\sum_{i,I} \frac{Z_I e^2}{|\mathbf{R}_I - \mathbf{r}_i|}\end{aligned} \tag{2.5}$$

This many-body problem is complicated to carry out and hence some approximations are applied to develop a theory that makes problem-solving feasible. The first approximation is the Born–Oppenheimer approximation which is based on the fact that the nuclei are much heavier than electrons and have relatively lower velocities. Relative to the time scale of nuclear motion, electrons instantaneously achieves their ground state configuration with

respect to nuclei. Hohenberg and Kohn [61] formulated DFT to determine the electronic ground state from first principles and thereby describing a many-electron system in an external potential ($V_{ext}(\mathbf{r})$). The Hamiltonian being:

$$\widehat{H} = -\frac{\hbar^2}{2m_e}\sum_i \nabla_i^2 + \sum_i V_{ext}(\mathbf{r}_i) + \frac{1}{2}\sum_{i,j(i\neq j)} \frac{e^2}{|\mathbf{r}_i - \mathbf{r}_j|} \tag{2.6}$$

The two Hohenberg–Kohn theorems which form the basis of DFT is summarized as follows:

1. For a system of interacting particles in an external potential ($V_{ext}(\mathbf{r})$), the ground state density of the particle $n_0(\mathbf{r})$, uniquely determines this potential except for a constant. Since ($V_{ext}(\mathbf{r})$) determines the $\widehat{H}$, it implies that $n_0(\mathbf{r})$ solely determines the total energy and all other properties of the system.

2. For any external potential ($V_{ext}(\mathbf{r})$), the total energy is a unique functional, $E[n]$, of the particle density $n(\mathbf{r})$. The ground state energy and density can be obtained by minimizing $E[n]$ with respect to changes in $n(\mathbf{r})$. The minimum of this functional is the ground state energy of the system and the density which minimizes the functional is the ground state density $n_0(\mathbf{r})$.

On employing DFT, the formulated problem are dealt with electron density rather $n(\mathbf{r})$ instead of wave function and the corresponding many-body Schrödinger equation. Thus, any ground state property of the material can be expressed as a functional of the electron density. Using the formalism of Hohenberg, and Kohn [61], Kohn, and Sham [63] derived a procedure yielding a set of equations whose solution is feasible with a self-consistent method. For a system in an external potential ($V_{ext}(\mathbf{r})$), the ground state energy can be expressed as a functional of the electron density:

$$E[n] = \int V_{ext}(\mathbf{r})n(\mathbf{r})d\mathbf{r} + F[n] \tag{2.7}$$

The term $F[n]$ other than known V_{ext} is a universal functional (independent of V_{ext}) and its form is unknown, however, it involves the kinetic energy of electrons and electron-electron

interactions that includes the Hartree energy:

$$\frac{1}{2}\int \frac{\mathrm{n}\left(\mathbf{r}\right)\mathrm{n}\left(\mathbf{r}'\right)}{|\mathbf{r}-\mathbf{r}|}\mathrm{d}\mathbf{r}\mathrm{d}\mathbf{r}' \tag{2.8}$$

For a non-interacting system of electrons in the external potential, F[n] is equal to the kinetic energy functional, $\mathrm{T_{ext}}$[n], and the single electron Schrödinger equations takes the form:

$$\left\{-\frac{1}{2}\nabla^2+\mathrm{V_{ext}}(\mathbf{r})\right\}\psi_{\mathrm{i}}(\mathbf{r})=\epsilon_{\mathrm{i}}\psi_{\mathrm{i}}(\mathbf{r});\ \mathrm{i}=1\ldots\mathrm{N} \tag{2.9}$$

with the density:

$$\mathrm{n}(\mathbf{r})=\sum_{\mathrm{i}=1}^{\mathrm{N}}|\psi_{\mathrm{i}}(\mathbf{r})|^2 \tag{2.10}$$

Therefore, the total energy corresponding to an interacting system of electrons can be expressed as:

$$E[\mathrm{n}]=\int \mathrm{V_{ext}}(\mathbf{r})\mathrm{n}(\mathbf{r})\mathrm{d}\mathbf{r}+\frac{1}{2}\int\frac{\mathrm{n}(\boldsymbol{r})\mathrm{n}\left(\mathbf{r}'\right)}{|\mathbf{r}-\mathbf{r}'|}\mathrm{d}\mathbf{r}d\mathbf{r}'+\mathrm{T_s}[\mathrm{n}]+\mathrm{E_{XC}}[\mathrm{n}] \tag{2.11}$$

where $\mathrm{E_{XC}}$[n] is known as exchange-correlation energy. The corresponding set of single particle equations for the N interacting electron system to be solved self consistently is:

$$\left\{-\frac{1}{2}\nabla^2+\mathrm{V_{eff}}(\mathbf{r})\right\}\psi_{\mathrm{i}}(\mathbf{r})=\epsilon_{\mathrm{i}}\psi_{\mathrm{i}}(\mathbf{r});\mathrm{i}=1\ldots\mathrm{N} \tag{2.12}$$

where the effective potential is

$$\mathrm{V_{eff}}=\mathrm{V_{ext}}(\mathbf{r})+\frac{1}{2}\int\frac{\mathrm{n(r)}}{|\mathbf{r}-\mathbf{r}'|}\mathrm{d}\mathbf{r}'+\mu_{\mathrm{XC}}(\mathrm{n}(\mathbf{r})) \tag{2.13}$$

with

$$\mu_{\mathrm{XC}}(\mathrm{n}(\mathbf{r}))=\frac{\delta\mathrm{E_x}[\mathrm{n}(\boldsymbol{r})]}{\delta\mathrm{n}(\mathbf{r})} \tag{2.14}$$

Solving the Kohn–Sham (KS) equations in self-consistent manner would yield the ground state energy and density of the interacting system of particles provided the functional $\mathrm{E_{XC}}$[n] is known. However, various reasonable approximations to the exchange-correlation energy ($\mathrm{E_{XC}}$[n]) have been adopted.

2.2.2 Solving Kohn-Sham equations

There are three basic approaches to expand the wave function in order to solve the KS equation describing an electron in an effective potential : (1) Plane wave basis sets, where the wave function and potential is developed using a large number of plane waves and involves Fourier transformation of real and reciprocal space. (2) Localized atomic-like orbitals (LCAOs) where the orbitals in the region close to atoms are of interest. (3) Atomic sphere methods where space is divided into a region close to atoms and regions between the atoms. The work presented in the thesis implements the plane waves and the pseudopotential method for solving the KS equations.

2.2.2.1 Self-consistent field method

The effective potential corresponding to the ground state electron density is obtained by solving the KS equations in a self-consistent way. The steps involved is illustrated in Fig. 2.1. At first, the charge density is initially guessed, $n_{in}(\mathbf{r})$, to calculate the effective potential ($V_{eff}(\mathbf{r})$). Using this charge density and potential, KS equations are solved to obtain the eigenstates from which new electronic charge density $n_{out}(\mathbf{r})$ is calculated. If the output potential and densities agree with the initial potential and densities, then one can proceed to the evaluation of total energy, forces, etc. otherwise the new density will be served as new input for constructing new $V_{eff}(\mathbf{r})$ and Hamiltonian which further yields new eigenstates and hence a new $n(\mathbf{r})$. This cycle is continued until self-consistency is achieved.

2.2.2.2 Plane waves

A crystal is made up of periodic arrangements of atoms and it can be generated by applying translation of a defined unit cell in three spacial directions. Therefore, the electrons experience a periodic potential. The periodicity of the lattice can be exploited for solving the KS equation by applying Bloch's theorem to each electronic wave function. According to Bloch's theorem, a wave function in a periodic lattice can be expressed as a product of a plane wave and a periodic function with the periodicity of the lattice.

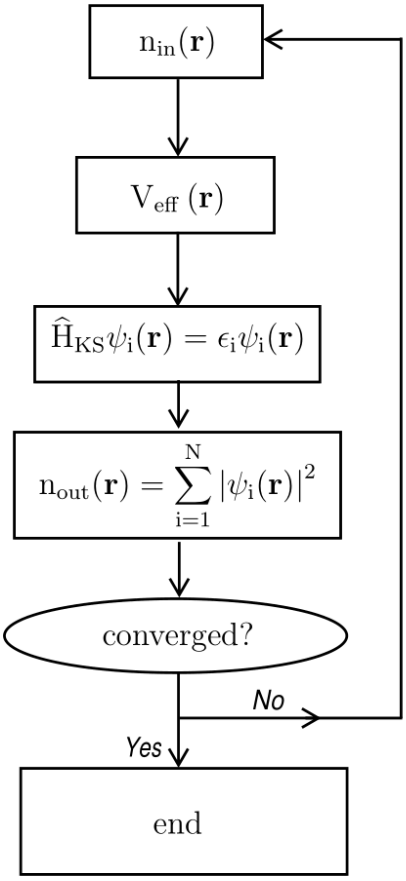

Figure 2.1: Flow chart describing the steps involved in a self-consistent field cycle for the solution of the KS problem.

Therefore, each electronic wave function can be written as a sum of plane waves:

$$\psi_{n,\boldsymbol{k}}(\mathbf{r}) = \sum_{\mathbf{G}} C_{n,\boldsymbol{k}+\mathbf{G}} e^{i(\boldsymbol{k}+\boldsymbol{G})\cdot\mathbf{r}} \tag{2.15}$$

where the summing index spans the reciprocal lattice vectors $\mathbf{G}$, $\mathbf{k}$ is a vector that identifies the state (spatial frequency) in the first Brillouin zone, C is the coefficient and 'n' is the band number.

2.2.2.3 Pseudopotential

Electrons in an atom experience two different kinds of potential. Those nearer to cores experience strong atomic potentials, and their wave function oscillates rapidly. The valence electron which majorly determines the properties of the system, however, experience a

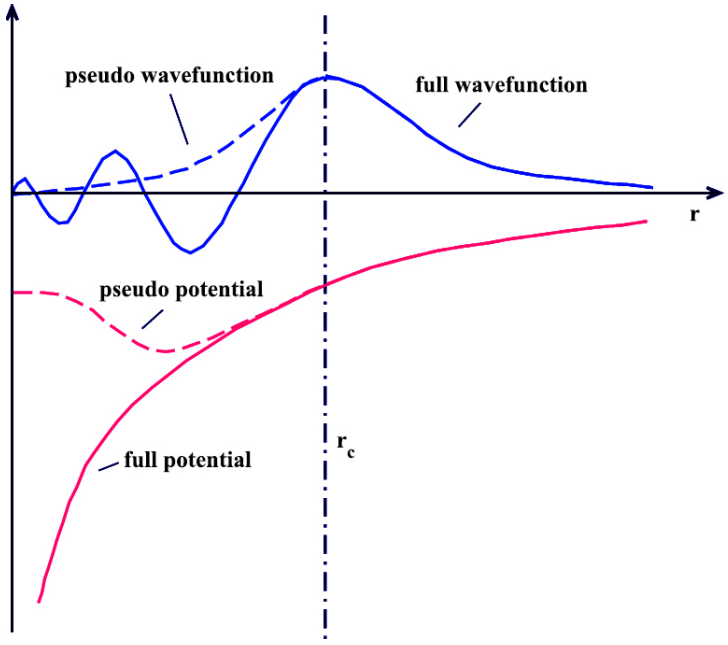

Figure 2.2: Illustration of the concept behind the pseudopotential. The pseudopotential and pseudo wave function coincides with the true valence wave function at the cut-off radius r_c and beyond.

smooth potential. For feasible calculations, the Coulomb potential due to the core electrons and nucleus are replaced by an effective pseudopotential that acts only on the valence electrons (see Fig. (2.2)). This pseudopotential and the pseudo wavefunction doesn't exhibit radial nodes in the core region wheras they behaves identical to real potential and wave function beyond a certain cutoff radius (r_c) that determines the boundary of core region. A few of the most employed pseudopotentials include norm-conserving pseudopotentials [64, 65], the projector-augmented wave pseudopotentials (PAWs) [66] and ultrasoft pseudopotentials [67].

2.2.2.4 k-point sampling

The determination of correct electron density and total energy requires considering all the **k**-vectors that corresponds to the occupied states. However, closely spaced **k**-points will have almost identical wave function, therefore, it is possible to use a finite set of **k**-points, called "special **k**-points" of a Brillouin zone to obtain accurate results. The **k**-point sampling performed for the work presented in this thesis employs Monkhorst–Pack scheme [68]. The error arising due to **k**-point sampling is minimized by using a denser

set of **k**-points which is achieved by performing a convergence test of total energy with **k**-points density.

2.2.2.5 Kinetic energy cut-off

In principle, Equation (2.15) states that an infinite number of plane waves is required to construct the electronic wave function. However, The coefficients $C_{\mathrm{n},\mathbf{k}+\mathbf{G}}$ for plane waves have kinetic energy $\frac{\hbar^2}{2m}|\mathbf{k}+\mathbf{G}|^2$, and the plane waves with smaller kinetic energy are more relevant than those having a very high kinetic energy. Hence, the size of the plane wave basis set can be reduced by including only those plane waves with kinetic energies lower than a cutoff energy value,E_{cutoff}:

$$\frac{\hbar^2}{2\ \mathrm{m}}|\mathbf{k}+\mathbf{G}|^2 < E_{\mathrm{cutoff}} \tag{2.16}$$

The error in the total energy due to this truncation of basis set can be minimized by increasing the energy cut-off which increases the size of the basis set and leads to convergence of total energy and other properties of the system.

2.2.3 Structural properties

2.2.3.1 Geometry relaxation

The total energy obtained after solving KS equations should be minimized with respect to atomic position, shape, and size of the unit cell to obtain the optimized structure. Atoms are said to be in a relaxed state when the forces acting on them are zero and it is necessary for having the optimized structure. The forces on the atoms are calculated using the Hellmann–Feynman theorem [69]. Further, the pressure on the system can be obtained from the stress tensor corresponding to each atomic configuration. The stress tensor is diagonal for hydrostatic pressure conditions. Hence, both forces on atoms and pressure in the system are obtained in a total energy calculation. If the stress tensor is not diagonal or the forces on atoms are not zero for a particular atomic configuration, then the atomic positions are changed by a minimization algorithm. The whole process of the self-consistency cycle and evaluation of force and stress is repeated for this new

atomic configuration until the forces on each atom obtained using the Hellmann–Feynman theorem are approximately zero.

2.2.3.2 Geometry optimization

For hydrostatic pressure, i.e if stress tensor (σ_{ij}) is diagonal, then in the ground state, the external pressure (P) is zero.

$$P - \frac{dE}{dV} = \frac{1}{3}(\sigma_{xx} + \sigma_{yy} + \sigma_{zz}) \tag{2.17}$$

Calculation of total energies for a different fixed volume of the unit cell is performed to obtain energy-volume curve E(V). The minimum of the curve corresponds to the atomic configuration with the lowest energy and therefore the equilibrium structure of the system. The pressure of the lowest energy structure will be zero. The E(V) curve can be fitted with an equation of states such as Birch-Murnaghan fit to obtain equilibrium volume, bulk modulus and pressure derivative of the bulk modulus. It should be noted that the thermal vibration of the system is neglected and the calculations are performed on fixed atomic positions. Hence, the simulations are performed at 0 K, and it doesn't include the zero-point vibrational contribution.

2.2.4 Vibrational and Mechanical properties

DFT only provides the ground state density and total energy, however, there are well-known failures in the representation of electronically excited states. If the ground state is perturbed very lightly, typically in such a manner as to leave the system close to its electronic ground state, one can easily apply the traditional quantum formalism for perturbation theory, giving density functional perturbation theory (DFPT). The goal of DFPT is to compute the derivatives of the DFT electronic energy with respect to different perturbations. The full derivation of the DFPT equations is found in Ref. [70–72].

2.2.4.1 Phonons

Under Born-Oppenheimer approximation, the nuclear and electronic degrees of freedom in the Hamiltonian can be decoupled and the computation of the total energy of the

system is done in two steps. At first, fixing the nuclei position in Equation (2.5) yield the Born-Oppenheimer Hamiltonian $\mathrm{H_{BO}}$ as:

$$\widehat{\mathrm{H}}_{\mathrm{BO}} = -\frac{\hbar^2}{2\mathrm{m}_e}\sum_i \nabla_i^2 + \frac{1}{2}\sum_{I,J(I\neq J)} \frac{Z_I Z_I e^2}{|\mathbf{R_I} - \mathbf{R_J}|} + \frac{1}{2}\sum_{i,j(i\neq j)} \frac{e^2}{|\mathbf{r_I} - \mathbf{r_J}|} - \frac{1}{2}\sum_{i,I} \frac{Z_I e^2}{|\mathbf{R_I} - \mathbf{r_i}|} \tag{2.18}$$

where $\mathrm{H_{BO}}$ depends parametrically upon the nuclear positions $\mathbf{R}$ and describes the problem of the interacting electrons moving in the electrostatic field of nuclei at fixed positions. The equation can be solved using DFT and ground-state Born-Oppenheimer energy can be obtained. To determine the lattice dynamics of the system, the kinetic energy of the nuclei is added to $\mathrm{E_{BO}}$ and the corresponding Schrödinger equation in Hartree atomic units ($\hbar = \mathrm{m}_e = e = 1/4\pi\epsilon_0 = 1$) becomes:

$$\left(-\frac{1}{2}\sum_{\mathrm{I}} \frac{1}{\mathrm{M_I}}\nabla_{\mathrm{I}}^2 + E_{\mathrm{BO}}(\mathbf{R})\right) = E\psi(\mathbf{R}) \tag{2.19}$$

where $\mathrm{M_I}$ are the masses of the atoms and E is the total energy. Let the vector '$\mathbf{T}$' represents the position of the unit cell with respect to the origin, 'I' represent a nucleus within the unit cell and α represents the cartesian directions. In principle, the nuclei undergo small displacement $\mathrm{u}_{\mathrm{I}\alpha}^{\mathrm{T}}$ about their equilibrium position $\mathbf{R}_{\mathrm{I}\alpha}^{\mathrm{T}}$. Therefore, the Born-Oppenheimer energy is expressed as a function of the nuclear displacements using a Taylor series expansion:

$$E_{\mathrm{BO}}(\mathrm{u}) = E_{\mathrm{BO}}^0 + \frac{1}{2}\sum_{\mathrm{TI}\alpha} \frac{\partial E_{\mathrm{BO}}}{\partial \mathbf{R}_{\mathrm{I}\alpha}^{\mathrm{T}}}\mathrm{u}_{\mathrm{I}\alpha}^{\mathrm{T}} + \frac{1}{2}\sum_{\mathrm{TI}\propto}\sum_{\mathrm{T'I'}\propto'} \frac{\partial^2 E_{\mathrm{BO}}}{\partial \mathbf{R}_{\mathrm{I}\alpha}^{\mathrm{T}} \partial \mathbf{R}_{\mathrm{I}\alpha'}^{\mathrm{T'}}}\mathrm{u}_{\mathrm{I}\alpha}^{\mathrm{T}}\mathrm{u}_{\mathrm{I'}\alpha'}^{\mathrm{T'}} + \cdots \tag{2.20}$$

where the first term $\mathrm{E_{BO}^0}$ is the minimum energy when the displacement is zero which can be calculated using standard DFT. The second term is the first derivative of the energy which represents forces acting on the atoms. At equilibrium, this force is zero ($\boldsymbol{F}_{\mathrm{I}\alpha}^{\mathrm{T}} = \frac{\partial E_{\mathrm{BO}}}{\partial \mathbf{R}_{\mathrm{I}\alpha}^{\mathrm{T}}} = 0$) and the first order term vanishes. The third term including the 2^{nd} derivative of the energy with respect to two atomic displacements is called the harmonic term and the Taylor expansion truncated after the harmonic term is referred as the harmonic approximation.

The higher-order terms in Equation (2.20) describe the anharmonic effects. The fourth and fifth terms are the first anharmonic term which gives the lifetimes of phonon and Raman/infrared peak widths. Under harmonic approximation, the restoring force acting on the nucleus depends linearly on the displacement of nuclei from the equilibrium position. The force on the nucleus 'I', due to the displacement of another nucleus I′ be expressed as:

$$\boldsymbol{F}^{\mathrm{T}}_{\mathrm{I}\alpha} = \frac{\partial E^{T}_{\mathrm{BO}}}{\partial \mathrm{u}^{\mathrm{T}'}_{\mathrm{I}'\alpha'}} = -\sum_{\mathrm{T}'\mathrm{I}'\beta'} \frac{\partial^2 E_{\mathrm{BO}}}{\partial \mathbf{R}^{\mathrm{T}}_{\mathrm{I}\alpha} \partial \mathbf{R}^{\mathrm{T}'}_{\mathrm{I}\alpha'}} \mathrm{u}^{\mathrm{T}'}_{\mathrm{I}'\alpha'} \tag{2.21}$$

Equation (2.21) has the one-to-one correspondence of elastic lattice where the force is expressed as $\mathrm{F} = -kx$, with k being the force constant and x being the displacement about the equilibrium position. Similarly, Equation (2.21) can be expressed as:

$$\boldsymbol{F}^{\mathrm{T}}_{\mathrm{I}\alpha} = -\sum_{\mathrm{T}'\mathrm{I}'\beta} \mathbf{C}_{\mathrm{I}\alpha,\mathrm{I}'\alpha'}\left(\mathrm{T},\mathrm{T}'\right) \mathrm{u}^{\mathrm{T}'}_{\mathrm{I}'\alpha'} \tag{2.22}$$

where $\mathbf{C}$ represents the matrix of interatomic force constants (IFC), consisting of elastic-like constants of all interatomic interactions:

$$\mathbf{C}_{\mathrm{I}\alpha,\mathrm{I}'\alpha'}\left(\mathrm{T},\mathrm{T}'\right) = \frac{\partial^2 E_{\mathrm{BO}}}{\partial \mathbf{R}^{\mathrm{T}}_{\mathrm{I}\alpha} \partial \mathbf{R}^{\mathrm{T}'}_{\mathrm{I}\alpha'}} \tag{2.23}$$

The equation of force following the Newtonian mechanics (Force = mass × acceleration) takes the form:

$$\boldsymbol{F}^{T}_{I\alpha}(\mathrm{t}) = \mathrm{M}_{\mathrm{I}} \frac{\partial^2 \mathbf{R}^{\mathrm{T}}_{\mathrm{I}\alpha}(\mathrm{t})}{\partial \mathrm{t}^2} \tag{2.24}$$

Equating the elastic force (Equation(2.22)) and Newtonian force (Equation(2.24)) force yields:

$$-\sum_{\mathrm{T}'\mathrm{I}'\beta} \boldsymbol{C}_{\mathrm{I}\alpha,\mathrm{I}'\alpha'}\left(\mathrm{T},\mathrm{T}'\right) \mathrm{u}^{\mathrm{T}'}_{\mathrm{I}'\alpha'} = \mathrm{M}_{\mathrm{I}} \frac{\partial^2 \mathbf{R}^{\mathrm{T}}_{\mathrm{I}\alpha}(\mathrm{t})}{\partial \mathrm{t}^2} \tag{2.25}$$

which further takes the form of a system of differential equations:

$$-\sum_{\mathrm{T}'\mathrm{I}'\alpha'} \boldsymbol{C}_{\mathrm{I}\alpha,\mathrm{I}'\alpha'}\left(\mathrm{T},\mathrm{T}'\right) \mathrm{U}^{\mathrm{T}'}_{\sigma}\left(\mathrm{I}',\alpha'\right) = \mathrm{M}_{\mathrm{I}}\omega^2_{\sigma} \frac{\partial^2 \mathbf{R}^{\mathrm{T}}_{\mathrm{I}\alpha}(\mathrm{t})}{\partial \mathrm{t}^2} \mathrm{U}^{\mathrm{T}}_{\sigma}(\mathrm{I}\alpha) \tag{2.26}$$

The solution for this set of equations in the harmonic approximation is a superposition of the normal modes of vibration of the system which represents a set of period elastic waves corresponding to atomic vibrations about their equilibrium positions with some specific frequencies. They are described as:

$$u_{\alpha}^{T}(t) = \sum_{\sigma} A_{\sigma} U_{\sigma}^{T}(I,\alpha) e^{i\omega_{\sigma} t} + c \tag{2.27}$$

where σ labels the normal modes, A_{σ} is their amplitude, ω_{σ} is their normal mode angular frequency, and 'c' is a constant. The pattern of the atomic displacements is set by $U_{\sigma}^{T}(I,\alpha)$. Since the lattice is periodic, the normal modes of vibration can be written as Bloch states, i.e. as the product of a plane wave and a function having a periodicity of the lattice:

$$U_{\sigma}^{T}(I,\alpha) = e^{i\mathbf{q}\cdot\mathbf{R}_{T}} U_{mq}(I,\alpha) \tag{2.28}$$

These nuclear displacements are quantized and are known as phonons. Phonon eigen displacements and their frequencies are obtained from diagonalization of a set of equations:

$$\sum_{I'\alpha'} D_{I\alpha I'\alpha'}(\mathbf{q}) U_{mq}(I',\alpha) = M_{I}\omega_{mq}^{2} U_{mq}(I,\alpha) \tag{2.29}$$

where $D_{I\alpha I'\alpha'}(\mathbf{q})$ is the dynamical matrices, which are the Fourier transforms of the interatomic force constants matrices at particular $\mathbf{q}$ vectors:

$$D_{I\alpha I'\alpha'}(\mathbf{q}) = \sum_{T'} \mathbf{C}_{I\alpha,I'\alpha}(0,T') e^{i\mathbf{q}\cdot\mathbf{R}_{T'}} \tag{2.30}$$

The IFCs and dynamical matrices are second order derivatives of the energy with respect to nuclear displacements, hence, they can be computed using DFPT. If the unit cell consists of N atoms, the dimension of the dynamical matrix is 3N×3N. Diagonalization of dynamical matrix yields eigenvalues, the square of the phonon frequencies, and eigen vector having 3N components. The eigen vector corresponds to the displacements of each nucleus along with the 3 cartesian directions. Phonon frequencies as a function of wavevector $\mathbf{q}$ form the dispersion relation and the corresponding plot form the phonon band structures.

2.2.4.2 Raman Spectrum

Raman spectroscopy provides a unique fingerprint of the environment and local bonding of materials. In Raman spectroscopy measurements of crystalline materials, laser photons with a frequency ω_{L}, interact with lattice vibrations, phonons. Photons that undergo inelastic scattering either exhibits a decrease or increase in frequency, resulting in symmetric stokes or anti-Stokes shifts, respectively. The intensity of the scattered photons is recorded as a function of frequency change known as Raman shifts. For theoretical calculations of Raman spectrum carried out in this thesis, the wavenumber of normal mode is obtained through phonon calculations employing DFPT. The intensity of the i^{th} mode with electric field along γ and polarization along β is given as [72]:

$$\mathrm{I}_{\mathrm{i}\beta\omega} = \frac{2\pi \mathrm{h}\left(\omega_{\mathrm{L}} - \omega_{\mathrm{i}}\right)^4}{\mathrm{c}^4 \omega_{\mathrm{i}}} \left[\mathrm{n}\left(\omega_{\mathrm{i}}\right) + 1\right] \alpha^2_{\mathrm{i}\beta\gamma} \tag{2.31}$$

where ω_{i} is the frequency of the vibrational mode, ω_{L} is the laser photon frequency which is arbitrarily set since the change in frequency of the scattered photon is independent of incident photon frequency due to the nature of the interaction. $\left[\mathrm{n}\left(\omega_i\right) + 1\right] = \left(1 - \mathrm{e}^{\frac{-h\omega_i}{k_B T}}\right)^{-1}$ is the Bose occupation number that depends on both frequency and temperature and $\alpha_{\mathrm{i}\beta\omega}$ is the Raman tensor for each mode which is obtained from the derivative of the dielectric tensor, $\epsilon_{\beta\gamma}$ with respect to the displacement $\mathrm{u}_{\mathrm{in}\nu}$:

$$\alpha_{\mathrm{i}\beta\omega} = \frac{\sqrt{\Omega}}{4\pi} \sum_{\mathrm{n,i},\gamma} \frac{\partial \epsilon_{\beta\gamma}}{\partial \mathrm{u}_{\mathrm{in}\nu}} \mathrm{e}_{\mathrm{in}\gamma} \mathrm{m}_{\mathrm{n}}^{-\frac{1}{2}} \tag{2.32}$$

where ν is the direction of displacement, m_{n} is the mass of atom 'n', $\mathrm{e}_{\mathrm{in}\gamma}$ is the eigenvector of the dynamical matrix and Ω is the volume of unit cell.

2.2.4.3 Elastic constants

Calculations of elastic constants can be performed once the structure is in equilibrium configuration which will be used as a reference system. The atomic positions are relaxed at every strain and the numerical derivative of the energy with respect to the strain yield the stress corresponding to the strained lattice. Therefore, stress as a function of strain is obtained, through which the elastic properties of a material can be determined. The

elastic constants which represents the second derivative of the energy with respect to the strain tensor for unit volume is given by:

$$\mathrm{C_{ijkl}} = \frac{\sigma_{\mathrm{ij}}}{\epsilon_{\mathrm{kl}}} \tag{2.33}$$

(where ϵ_{kl} and σ_{ij} represents the components of the strain and stress tensor respectively). The set of $\mathrm{C_{ijkl}}$ can be expressed as a 6×6 matrix of independent elastic constants, $\mathrm{C_{ij}}$ and the number of $\mathrm{C_{ij}}$ is determined by the symmetry of the crystal. Bulk, shear, and Young modulus can be determined using appropriate averaging approaches such as proved by Reuss, Voight and Hill [73]. In particular, the bulk and shear modulus in the Voigt approach are:

$$\mathrm{B_V} = \frac{1}{9}\left[(c_{11} + c_{22} + c_{33}) + 2\,(c_{12} + c_{23} + c_{13})\right] \tag{2.34}$$

$$\mathrm{G_V} = \frac{1}{15}\left[(c_{11} + c_{22} + c_{33}) - (c_{12} + c_{23} + c_{13}) + 3\,(c_{44} + c_{55} + c_{66})\right] \tag{2.35}$$

and for the Reuss approach are:

$$\mathrm{B_R} = \frac{1}{9}\left[(\sigma_{11} + \sigma_{22} + \sigma_{33}) + 2\,(\sigma_{12} + \sigma_{13} + \sigma_{23})\right] \tag{2.36}$$

$$\mathrm{G_R} = \frac{1}{15}\left[(\sigma_{11} + \sigma_{22} + \sigma_{33}) - (\sigma_{12} + \sigma_{13} + \sigma_{23}) + 3\,(\sigma_{44} + \sigma_{55} + \sigma_{66})\right] \tag{2.37}$$

Hill [74] shown that the Voigt and Reuss aproaches serve as upper and lower bound for elastic moduli respectively. Thus, the Hill-averaged bulk and shear moduli are given as:

$$\mathrm{B_H} = \frac{1}{2}\left(\mathrm{B_V} + \mathrm{B_R}\right) \tag{2.38}$$

$$\mathrm{G_H} = \frac{1}{2}\left(\mathrm{G_V} + G_{\mathrm{R}}\right) \tag{2.39}$$

Using bulk modulus, B, and the shear modulus, G one can obtain Young modulus, E, and the Poisson ratio, ν, as:

$$\mathrm{E} = \frac{9BG}{3B + G} \tag{2.40}$$

$$v = \frac{3\mathrm{B} - 2\mathrm{G}}{2(3\mathrm{B} + \mathrm{G})} \tag{2.41}$$

2.3 Experimental Methods

2.3.1 X-ray diffraction

X-ray diffraction (XRD) is a non-destructive and versatile analytical technique that provides detailed structural and phase information of geological materials explored in a research laboratory. For example, the density and compressibility of mantle materials have been determined widely using XRD. In principle, XRD measurements constrain the crystal structure and lattice parameters of the sample. Measuring the unit cell volume of the sample as a function of pressure can be fitted using an appropriate equation of state yield bulk modulus, and its pressure derivative at ambient conditions. From the X-ray diffraction data, inter-planar spacing of different lattice planes (hkl) can be determined from which the crystal structure of the material can be solved by Rietveld refinement. X-rays are scattered by atoms in all directions. Since the arrangement of the atom is periodic in a crystal, the scattered X-rays exhibit a certain phase relationship. The phase relationship is such that, in most of the directions, the scattered wave undergoes destructive interference whereas in few directions, constructive interference occurs forming diffracted beams. Consider the X-rays reflected from a set of lattice planes with inter-planar spacing d in a crystal as shown in Fig. (2.3). The scattered X-rays will undergo constructive interference if the path difference of ray paths ABC and A′B′C′ is equal to an integer (n) multiple of the wavelengths. This general relationship between the angle of incidence, wavelength of the incident X-rays and spacing between the crystal lattice planes of atoms is known as Bragg's Law and is expressed as:

$$n\lambda = 2d\sin\theta \tag{2.42}$$

where λ is the wavelength of the incident X-rays, d is the interplanar spacing of the crystal and θ is the angle of incidence, n is called the order of diffraction and is equal to the number of wavelengths in the path difference between rays scattered by adjacent planes. For fixed values of d and λ, diffraction may occur at several angles of incidence $\theta_1, \theta_2, \theta_3...$ corresponding to $n = 1, 2, 3...$ Bragg equation can also be expressed in terms of energy. Wavelength in terms of energy can be expressed as: $\lambda = hc/E$, where c is the speed of

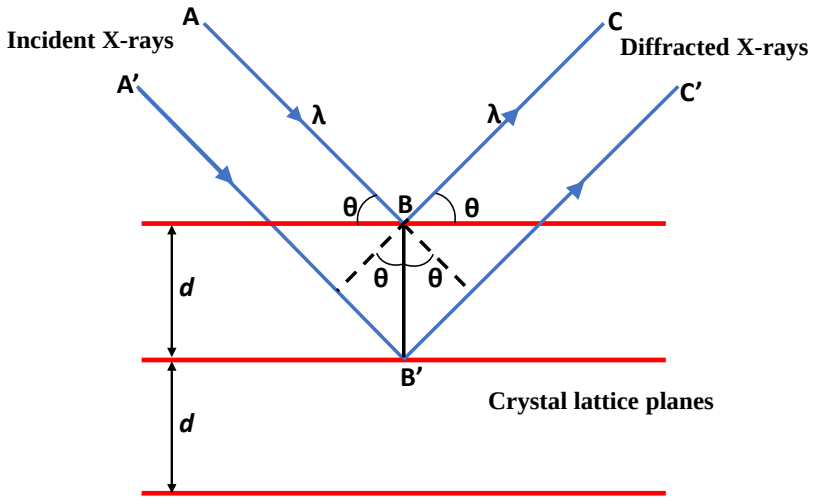

Figure 2.3: Schematic representation of Bragg's Law of reflection. Constructive interference occurs when the difference between the incident ray path ABC and diffracted ray path A′B′C′ differs by an integer number of wavelengths (λ).

light,h is the Planck's constant, and E is the energy of the photon. Therefore, the Bragg equation can also takes the form as:

$$E(\text{keV}) = 6.199/(d(\text{in}\text{Å})\sin\theta) \tag{2.43}$$

The most common X-ray diffraction technique in high-pressure research is powder diffraction. The high-pressure X-ray powder diffraction (XRPD) measurements can be carried out by the angle-dispersive method (ADXRD) or the energy-dispersive method (EDXRD). In the ADXRD method, monochromatic X-rays are used where the diffraction patterns are recorded using an area detector with spacial resolution (called 2D detectors) while fixing the energy of the X-ray as shown in Fig. 2.4(a). According to the Bragg equation (Equation (2.42)), diffraction angle determines the d-spacings of different lattice planes (hkl). In the EDXRD configuration, polychromatic X-rays are used as radiation source, and the scattered photons from the sample are detected by a solid-state detector (SSD) having energy resolution. The detector is kept at a fixed angle, 2θ as shown in Fig. 2.4(b). In this case, the energy of the scattered photon determines the d-spacing according to the Bragg equation (Equation (2.43)).

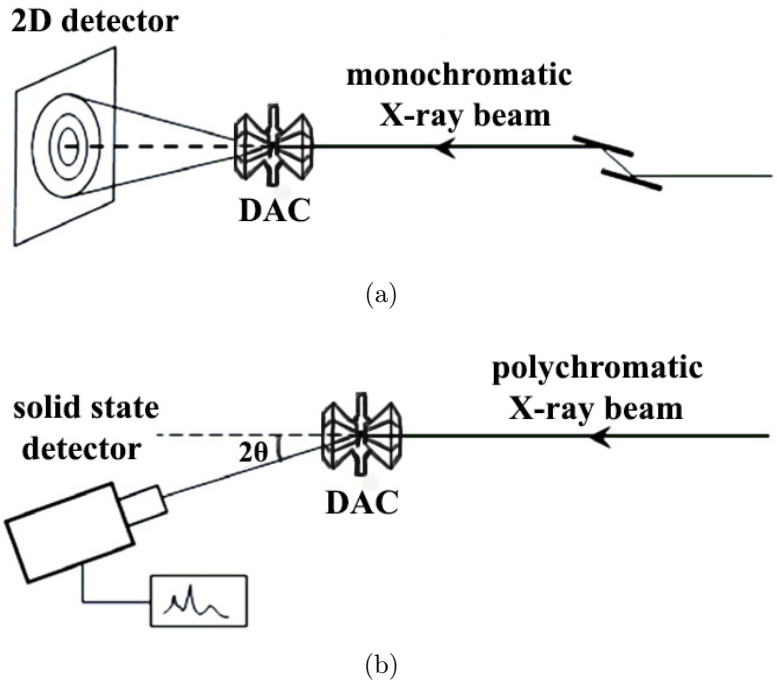

Figure 2.4: Schematic representation of diffraction geometry using DAC (a) ADXRD and (b) EDXRD (Ref. [75])

2.3.2 Synchrotron X-ray diffraction

Compared with typical laboratory sources, synchrotrons provide high-energy X-rays that substantially reduce the acquisition times required. For high-pressure studies, the X-rays emitted from a synchrotron radiation (SR) source are generally preferred. The high collimation and brightness of SR allow the X-ray beams focus on the micrometer-sized area for investigating minute amount samples at ultrahigh-pressures. Further, the high energy of SR enables it to penetrate the surrounding materials and suppress signals from the background, which is crucial for yielding high-quality diffraction data. The widely used high-pressure device for XRD is the diamond anvil cell (DAC) which is transparent to X-ray radiation and is capable of generating pressures beyond 400 GPa [76, 77]. The high-pressure studies carried out in this thesis were performed at Xpress beamline at the Elettra Sincrotrone, Trieste [78]. Xpress is a dedicated high-pressure diffraction beamline, employing a monochromatic X-ray beam of energy 25 keV focused on a large area detector for collecting diffraction data in angle dispersive mode. This configuration allows high-pressure powder diffraction experiments using diamond anvil cells (DAC)

where the in-situ pressure monitoring is done by an online ruby fluorescence spectrometer.

2.3.3 The working of diamond anvil cell

Diamond anvil cells (DAC) are widely used to pressurize samples due to their simplicity, performance, and safety. The DAC belongs to a class of high-pressure devices called opposed anvil devices that creates high-pressures by compressing a sample between tiny flat faces of the tip of two diamonds (culet faces) (see Fig. 2.5). The diamond anvils are supported by 'seats' which transmit the pressure from the rest of the cell to the diamonds. The anvils are perfectly aligned to avoid high-stress state in the diamonds which can fracture the anvils. Once compressed, high-pressure is generated at the centre of the sample. However, the sample edges will be at atmospheric pressure which causes a large pressure gradient within the sample. Because the edges of the sample are at 1 atmosphere, there is a tremendous pressure gradient within the sample. The high-pressure at the centre is accompanied by the shear stress and friction between the diamond face and the sample. For studies requiring hydrostatic conditions, gaskets and pressure transmitting media are used. The gasket is pierced with a hole that serves as a high-pressure chamber for experimental volume. When the anvils squeeze the gasket, it undergoes plastic deformation and reduces the volume of the hole which builds up pressure in the sample. The mechanism of applying pressure is the process of tuning the distance between the diamonds and keeping them stable at that position, where springs and screws are usually used to apply force to the seats of the diamond anvil.

At synchrotrons, where the pressure control must be managed remotely, the springs are replaced by a membrane control or motorized pressure control. The measurement of pressure generated in the sample is usually done using two strategies: 1) Measuring the unit cell volume of a material whose equation of state (EoS) is well known or 2) Measuring the position of the fluorescence lines of yttrium aluminium garnet or Ruby, positions of which are known as a function of pressure. The most commonly used pressure measurement strategy is measuring the fluorescence line of ruby, as ruby is chemically inert and has strong fluorescence in exposure to green laser light. For the high-pressure XRPD measurements carried out in the work presented in this thesis, a membrane DAC

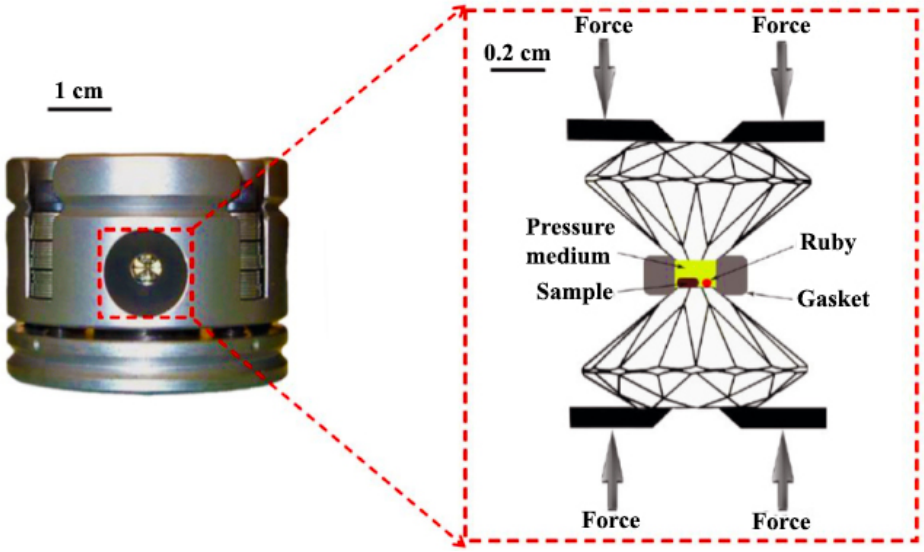

Figure 2.5: Schematic view of components that assembles to form a DAC (Ref. [79]).

with diamonds having culet size of 500 microns were used to apply the pressure. The sample chamber was prepared by pre-indenting a steel gasket of 200-micon thickness to about 80 microns and a hole having a diameter of 160 micron was prepared at the center. An automatic membrane pressure drive was used to apply the pressure.